molecular pharmaceutics

ARTICLE

pubs.acs.org/molecularpharmaceutics

Targeted Delivery of Cargoes into a Murine Solid Tumor by a Cell-Penetrating Peptide and Cleavable Poly(ethylene glycol) Comodified Liposomal Delivery System via Systemic Administration

Rui Kuai,[†,§] Wenmin Yuan,[†,§] Wanyu Li,[‡] Yao Qin,[†] Jie Tang,[†] Mingqing Yuan,[†] Ling Fu,[†] Rui Ran,[†] Zhirong Zhang,[†] and Qin He*[,†]

[†]Key Laboratory of Drug Targeting and Drug Delivery Systems, Ministry of Education, West China School of Pharmacy, Sichuan University, Chengdu, Sichuan, P. R. China

[‡]Pharmacy College of Chongqing Medical University, Chongqing, P. R. China

Supporting Information

ABSTRACT: A liposomal delivery system with a high efficiency of accumulation in tumor tissue and then transportation of the cargo into tumor cells was developed here and evaluated via systemic administration. 1,2-Distearoyl-*sn*-glycero-3-phosphoethanolamine-poly(ethylene glycol)$_{2000}$ (DSPE-PEG$_{2000}$)-TAT and protective DSPE-PEG$_{2000}$ modified liposomes possessing good stability in 50% FBS (fetal bovine serum) and good uptake efficiency were used as the basic formulation (TAT-SL; SL = stealth liposome), and then longer cysteine (Cys)-cleavable PEG$_{5000}$ was incorporated to modulate the function of TAT. All of the formulations to be used *in vivo* had sizes in a range of 80−100 nm and were stable in the presence of 50% FBS. Optical imaging showed that the incorporation of cleavable PEG$_{5000}$ into TAT-SL (i.e., C-TAT-SL) led to much more tumor accumulation and much less liver distribution compared with TAT-SL. The *in vivo* delivery profiles of C-TAT-SL were investigated using DiD as a fluorescent probe. Confocal laser scanning microscopy and flow cytometry showed that C-TAT-SL had a 48% higher ($p < 0.001$) delivery efficiency in the absence of Cys and a 130% higher ($p < 0.001$) delivery efficiency in the presence of Cys than the control (SL), indicating the successful targeted delivery of cargo was achieved by C-TAT-SL via systemic administration especially with a subsequent administration of Cys.

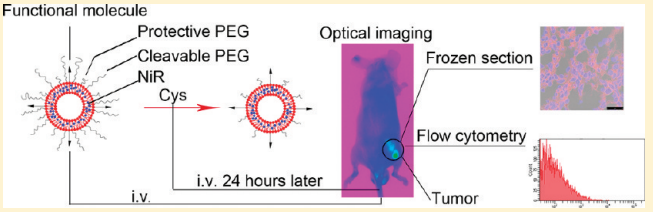

KEYWORDS: liposomes, cleavable PEG, TAT, distribution, targeted delivery

1. INTRODUCTION

Nowadays, cancer has become one of the greatest threats to the health of human beings; thousands of people die of cancer each year. Technology that could achieve tumor targeted delivery of cargo from low molecular weight drugs to macromolecules such as proteins and nucleic acids is in great need for its application on the diagnosis and treatment of tumors.[1−3] Various nanocarriers such as liposomes, nanoparticles, dendrimers, and micelles have been used to achieve this goal. Liposomes exhibited obvious advantages for their natural components, good biocompatibility, and good protection for the contents and tunable pharmacokinetics.[4−9]

In our previous study, the combination of a trans-activating transcriptional activator (TAT) and cleavable poly(ethylene glycol) (PEG) in the liposomes showed good delivery performance *in vitro* and *in vivo* via the intratumoral injection.[10] In this research, the delivery system was further optimized before the systemic use.

It is well-known that PEG coating could make the liposomes become "stealth liposomes" (SLs), evading the trapping of the reticuloendothelial system (RES) and endowing the liposomes with long circulating properties; thus there is a better chance for liposomes to extravasate from the bloodstream into tumor tissue via the enhanced permeability and retention (EPR) effect.[11] However, PEG coating is not always favorable in the whole process of tumor targeted delivery; it can hinder the direct interaction between liposomes and tumor cells after accumulation in tumor.[12] To improve the cellular uptake, incorporation of a "functional molecule"—TAT—on the distal end of a PEG spacer is an efficient method.[13−18] It was reported the uptake efficiency was highly related to the density of TAT on the surface of liposomes, and the density of TAT could in turn affect the size, aggregation characteristics in serum, and biodistribution profiles.[19] Moreover, the exposed TAT could penetrate various cells encountered without any specificity, and like other ligands it was easy to bind to opsonin in the blood and was then trapped by the liver, especially at high density, which was unfavorable for its

Received: March 1, 2011
Accepted: October 9, 2011
Revised: August 31, 2011
Published: October 10, 2011

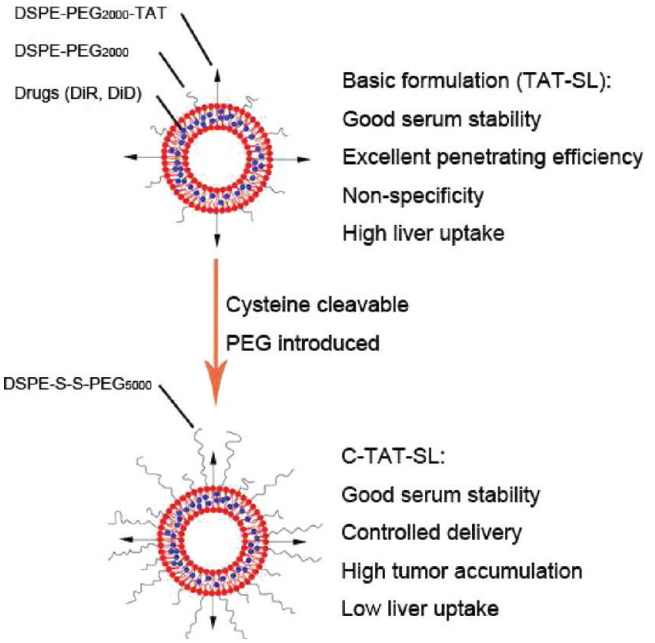

Figure 1. Schematic illustrations of TAT-SL, TAT and cleavable PEG comodified liposomal system (C-TAT-SL).

tumor targeting via systemic use.[20] Its function needed to be switched off during circulation; thus, any undesired uptake or binding of opsonin could be minimized and switched on after accumulation in tumor tissue, all of which could be achieved by the incorporation of cleavable PEG.[21−27]

In this study, an optimized liposomal delivery system (Figure 1) suitable for the systemic administration was designed based on the above details: 1,2-distearoyl-*sn*-glycero-3-phosphoethanolamine-poly(ethylene glycol)$_{2000}$ (DSPE-PEG$_{2000}$)-TAT as well as protective DSPE-PEG$_{2000}$ was used to modify liposomes: the former could enhance the ability of entering cells, while the latter could improve the serum stability of liposomes. Liposomes possessing both good stability in the presence of 50% FBS and good uptake efficiency were used as the basic formulation (TAT-SL), and then longer cysteine (Cys)-cleavable PEG$_{5000}$ (DSPE-S-S-PEG$_{5000}$) was incorporated into the basic formulation to tune the function of TAT. It was reported the concentration of a reducing agent such as Cys and glutathione was low in the body,[24] DSPE-S-S-PEG$_{5000}$ was stable enough to endue liposomes with plenty of time to accumulate in the tumor. In this optimized system, TAT could be shielded by the longer cleavable PEG spacer during circulation,[15] whose function was switched off. After the tumor accumulation was achieved, a safe reducing agent—Cys—was injected, and the longer cleavable PEG spacer could dissociate from the surface of liposomes. The function of TAT was switched on, and then efficient delivery of liposomal cargo occurred.

2. MATERIALS AND METHODS

2.1. Materials. Soy phosphatidylcholine (SPC) was obtained from Chengdu Kelong Chemical Company. 1,2-Distearoyl-*sn*-glycero-3-phosphoethanolamine (DSPE), 1,2-distearoyl-*sn*-glycero-3-phosphoethanolamine-poly(ethylene glycol)$_{2000}$ (DSPE-PEG$_{2000}$), 1,2-distearoyl-*sn*-glycero-3-phosphoethanolamine-poly(ethylene glycol)$_{2000}$-maleimide (DSPE-PEG$_{2000}$-Mal), and 1,2-dimyristoyl-*sn*-glycero-3-phosphoethanolamine-*N*-(lissamine rhodamine B sulfonyl) (ammonium salt) (Rh-PE) were purchased from Avanti Lipids. PEG$_{5000}$-SH and PEG$_{5000}$-NHS were obtained from Jenkem Technology (Beijing, China). TAT peptide with a terminal cysteine (Cys-AYGRKKRRQRRR) was provided by Chengdu KaiJie Biopharmaceutical Co., Ltd. (Chengdu, China). *N*-Succinimidyl-3-(2-pyridyldithio) propionate (SPDP) was purchased from Sigma (China, mainland). 1,1′-Dioctadecyl-3,3,3′,3′-tetramethylindotricarbocyanine iodide (DiR) and 1,1′-dioctadecyl-3,3,3′,3′-tetramethylindodicarbocyanine 4-chlorobenzenesulfonate salt (DiD) were purchased from Biotium. Collagenase type IV and DNase I were purchased from Biosharp. Other chemicals and reagents were of analytical grade and used without further purification.

2.2. Synthesis of DSPE-PEG$_{2000}$-TAT. DSPE-PEG$_{2000}$-TAT was synthesized in the aqueous phase as described previously with some modification.[14] Briefly, chloroform was removed from DSPE-PEG$_{2000}$-Mal (1 equiv) solution by rotary evaporation, and the obtained thin film was kept in vacuum over 4 h to remove the residual solvent. Then the thin film was hydrated in phosphate-buffered saline (PBS; pH 7.4) in a bath-type sonicator for about 1 min, and TAT peptide (3 equiv) in PBS (pH 7.4) was added into the micelle solution. The mixture was allowed to react at 4 °C under nitrogen for about 48 h. The excess TAT was removed by passing through a Sephadex-G50 (Pharmacia) column. The collected micelle solution was freeze-dried and then extracted by chloroform twice to remove the inorganic salts.

2.3. Synthesis of DSPE-S-S-PEG$_{5000}$/DSPE-PEG$_{5000}$. The synthesis of DSPE-S-S-PEG$_{5000}$ was performed as described previously with some modification.[9,10,24] Briefly, DSPE (0.1 equiv) was added into chloroform (55 °C) containing triethylamine (0.645 equiv), and then SPDP (0.08 equiv) was added. The mixture was allowed to react freely at room temperature under argon. After thin-layer chromatography (TLC) showed the disappearance of SPDP, PEG$_{5000}$-SH (0.035 equiv) was added, and the mixture again was allowed to react for about 72 h. The product was purified by chromatography on silica column before use.

DSPE-PEG$_{5000}$ was synthesized by reacting PEG$_{5000}$-NHS (1 equiv) with DSPE (1.5 equiv) in chloroform. The excess DSPE was precipitated by adding acetonitrile and then removed by centrifugation. Each PEG lipid was stored at −20 °C until use.

2.4. Preparation of Liposomes. A thin lipid film was obtained by rotary evaporation of chloroform from a lipid mixture indicated in Tables 1 and 2. The basic composition was SPC/Cho = 65:35, and the percentage of SPC decreased with the addition of various PEG-lipid derivatives. For the cellular uptake *in vitro*, 0.3% mol of Rh-PE was added; for the optical imaging of tumor bearing mice, a near-infrared lipophilic fluorescent dye, DiR, was added at a final concentration of 20 μg/mL to trace the location of liposomes and to determine the cellular uptake *in vivo* qualitatively and quantitatively, an analogue of DiR, lipophilic DiD, was added at a final concentration of 20 μg/mL. The obtained thin film was kept in vacuum over 4 h to remove the residual chloroform then hydrated using PBS (pH 7.4) in a bath-type sonicator for 2 min and intermittently sonicated by using a probe sonicator at 60 W for 75 s.

2.5. Characterization of Liposomes. The size and zeta potential of the liposomes in PBS (pH7.4) were measured by a Malvern Zetasizer Nano ZS 90 instrument (Malvern Instruments Ltd., U.K.).

The aggregation characteristic of liposomes was performed as reported by Oku et al.[28] The liposomal solution (2 mg/mL

Table 1. Compositions of Different Formulations of Liposomes and Their Size and Zeta Potential

composition	SPC (μmol)	Cho (μmol)	DSPE-PEG_{2000} (μmol)	DSPE-PEG_{2000}-TAT (μmol)	size[a] (nm)	zeta[a] (mV)
2% TAT + 0% PEG_{2000}	6.30	3.50	0.00	0.20	98.04 ± 4.84	7.8 ± 1.3
2% TAT + 1% PEG_{2000}	6.20	3.50	0.10	0.20	97.11 ± 2.06	7.6 ± 1.2
2% TAT + 2% PEG_{2000}	6.10	3.50	0.20	0.20	95.18 ± 5.56	7.4 ± 2.6
2% TAT + 3% PEG_{2000}	6.00	3.50	0.30	0.20	96.77 ± 2.43	6.4 ± 2.6
2% TAT + 4% PEG_{2000}	5.90	3.50	0.40	0.20	95.37 ± 1.33	3.5 ± 1.6
2% TAT + 5% PEG_{2000}	5.80	3.50	0.50	0.20	92.00 ± 3.68	3.6 ± 1.0
1% TAT + 0% PEG_{2000}	6.40	3.50	0.00	0.10	99.22 ± 0.21	3.6 ± 1.2
1% TAT + 1% PEG_{2000}	6.30	3.50	0.10	0.10	95.47 ± 0.64	3.4 ± 1.4
1% TAT + 2% PEG_{2000}	6.20	3.50	0.20	0.10	95.11 ± 1.48	2.5 ± 1.2
1% TAT + 3% PEG_{2000}	6.10	3.50	0.30	0.10	94.36 ± 3.56	1.9 ± 2.4
1% TAT + 4% PEG_{2000}	6.00	3.50	0.40	0.10	93.48 ± 1.23	1.3 ± 2.1
1% TAT + 5% PEG_{2000}	5.90	3.50	0.50	0.10	91.17 ± 1.75	0.9 ± 0.5
0.5% TAT + 0% PEG_{2000}	6.45	3.50	0.00	0.05	98.64 ± 1.92	0.1 ± 1.7
0.5% TAT + 1% PEG_{2000}	6.35	3.50	0.10	0.05	95.81 ± 0.12	0.1 ± 0.3
0.5% TAT + 2% PEG_{2000}	6.25	3.50	0.20	0.05	95.85 ± 3.17	0.6 ± 0.8
0.5% TAT + 3% PEG_{2000}	6.15	3.50	0.30	0.05	96.18 ± 0.75	1.0 ± 0.4
0.5% TAT + 4% PEG_{2000}	6.05	3.50	0.40	0.05	93.13 ± 1.74	0.7 ± 0.6
0.5% TAT + 5% PEG_{2000}	5.95	3.50	0.50	0.05	92.76 ± 5.38	0.3 ± 0.5

[a] Data represent mean ± SD(n = 3).

Table 2. Compositions of Different Liposomes and Their Abbreviations

	corresponding compositions		
abbreviations	SPC	Cho	functional lipids composition
SL	62.0%	35.0%	3% PEG_{2000}
TAT-SL	61.5%	35.0%	0.5% TAT/3% PEG_{2000}
C-TAT-SL	53.5%	35.0%	8% DSPE-S-S-PEG_{5000}/0.5% TAT/ 3% PEG_{2000}
N-TAT-SL	53.5%	35.0%	8% DSPE-PEG_{5000}/0.5% TAT/ 3% PEG_{2000}
C-SL	54.0%	35.0%	8% DSPE-S-S-PEG_{5000}/3% PEG_{2000}

lipids) was incubated in the presence of 50% FBS at 37 °C for 24 h. The turbidity (indicated by transmittance, T%) of the mixture was measured at 750 nm. The relative turbidity indicated by the transmittance of samples/transmittance of 50% FBS was used to characterize the extent of aggregation.

2.6. Cell Culture. C26 cells (a murine colon tumor cell line) were grown in RPMI-1640 medium (GIBCO) containing 10% FBS, 100 μg/mL streptomycin, and 100 U/mL penicillin. The cells were maintained at 37 °C in a humidified incubator with 5% CO_2.

2.7. Cellular Uptake Characteristic *in Vitro*. The cellular uptake characteristic measurement was performed as described previously.[29] Briefly, C26 cells were seeded on 24-well plates at a density of 1.5×10^5 cells/well 24 h before use. Each formulation of liposome was added at 50 μL/well in triplicate with PBS or various amounts of L-Cys (2.5, 5, 10, 20 mM) added at the same time. After incubation at 37 °C under 5% CO_2 for 4 h, the cells were washed by PBS and observed under fluorescence microscopy (Axiovert 40 CFL, Carl Zeiss Shanghai Co., Ltd.). Then the cells were added with 500 μL/well of 1% Triton-X100 at 4 °C over 2 h, and 100 μL of the lysate was used for the quantitative determination of the total protein of cells using the BCA assay kit (pierce), and the rest was used to determine the cell-associated fluorescence on a spectrofluorimeter (RF-5301 fluorospectrophotometry, Shimadzu, Japan) at a wavelength of Ex = 560 nm and Em = 578 nm. The uptake efficiency was indicated as fluorescence intensity/μg protein.

2.8. Tumor-Bearing Mice Model. Male BALB/c weighing about 20 g were purchased from the Experiment Animal Center of Sichuan University (P.R. China). All of the animal experiments adhered to the principles of care and use of laboratory animals and were approved by the Experiment Animal Administrative committee of Sichuan University.

Tumor-bearing mice were established as described previously.[30−33] Briefly, about 2×10^6 tumor cells were subcutaneously injected in the left flank of the mice. Tumors were allowed to grow to an average size of about 10 mm in diameter before the experiment.

2.9. *In Vivo* Biodistribution in Tumor Bearing Mice. On day 14 after tumor inoculation, the *in vivo* biodistribution experiment was performed using a noninvasive optical imaging method.[34−38] Mice were sheared thoroughly to exclude the interference of hair before different formulations of DiR loaded liposomes (2 mg lipids/mL) were injected at a dose of 20 mg lipids/kg via the tail vein. At 6, 24, 48, and 72 h postinjection, the whole body optical imaging was taken using a Kodak In-Vivo FX Professional Imaging System (New Haven, CT) with a wavelength set at Ex = 770 nm, Em = 830 nm and an exposure time of 20 s. Before each imaging the mice were anesthetized by an intra-abdominal injection of 8% chloral hydrate (400 mg/kg). The imaging was processed using Kodak MI software 5.0.1.

2.10. Qualitative and Quantitative Determination of Delivery Efficiency *in Vivo*. To investigate the delivery efficiency of different formulations of liposomes *in vivo* qualitatively, an analogue of DiR, DiD, was encapsulated into different formulations of liposomes (2 mg lipids/mL) as described above and injected at a dose of 20 mg lipids/kg via the tail vein. About 24 h later, PBS (pH 7.4) or Cys in PBS (30 mg/mL) was injected via

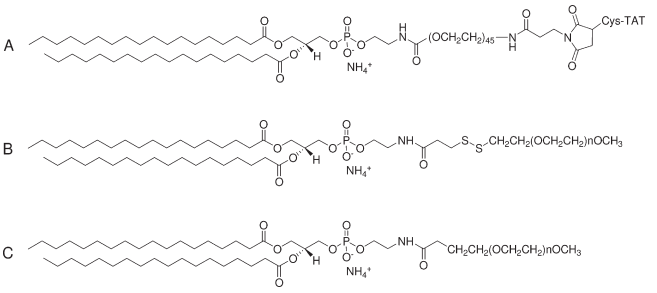

Figure 2. Chemical structure of DSPE-PEG$_{2000}$-TAT (A), DSPE-S-S-PEG$_{5000}$ (B), and DSPE-PEG$_{5000}$ (C).

the tail vein at a dose of 4 mL/kg to evaluate the effect of Cys on the delivery *in vivo*. Four hours later, mice were killed by cervical dislocation, and tumors were excised and frozen sectioned (4 μm in thickness). Sections were stained with DAPI (2 μg/mL), washed three times with cold PBS, and then observed using a Leica TCS SP5 AOBS confocal microscopy system (Leica, Germany).

To reveal the delivery efficiency in the entire tumor *in vivo*, the quantitative determination was performed as reported previously.[24,39] Briefly, tumors were excised and cut into small pieces of 2−4 mm and then treated with dissociation solution [collagenase type IV (1 mg/mL) and DNase I(30 μg/mL) in PBS] for 30 min at 37 °C with gentle shaking; then it was passed through 70-μm mesh. The obtained cell suspension was centrifuged at 4 °C, and cell pellets were washed three times with PBS and finally resuspended in PBS for flow cytometry measurement. Flow cytometry was done using the APC channel for DiD, and tumor cells from tumor-bearing mice receiving blank PBS served as blank. At least 10 000 cells were collected per sample. The results were indicated as the mean fluorescence intensity.

2.11. Statistical Analysis. Statistical comparisons were performed by one-way ANOVA for multiple groups, and a p value <0.05 was considered to be indicative of statistical significance.

3. RESULTS

3.1. Synthesis of DSPE-PEG$_{2000}$-TAT/DSPE-S-S-PEG$_{5000}$/DSPE-PEG$_{5000}$. Time-of-flight electrospray mass spectrometry (TOF MS ES+) confirmed the formation of DSPE-PEG$_{2000}$-TAT (M_w observed = 4570 Da). The chemical structure of DSPE-S-S-PEG$_{5000}$ and DSPE-PEG$_{5000}$ was confirmed by ^{1}H NMR (data not shown; structures shown in Figure 2) and TOF MS ES+ (6010 Da for DSPE-S-S-PEG$_{5000}$ and 5907 Da for DSPE-PEG$_{5000}$, respectively). Each PEG lipids had purity over 90% indicated by TLC.

3.2. Liposome Characterization. It was reported that the size of liposomes, especially aggregation sizes in the presence of serum, is one of the most important factors governing the fate of liposomes *in vivo*.[28] As shown in Table 1, liposomes containing various amounts of DSPE-PEG$_{2000}$ and DSPE-PEG$_{2000}$-TAT had sizes between 90 and 100 nm and zeta potentials mainly in the range of 0−10 mV. The aggregation characteristics in PBS or FBS were investigated subsequently. No increase in turbidity (indicated by the decrease of transmittance, T%) was observed after 24 h in PBS for all formulations (data not shown), but turbidity did increase after 24 h in the presence of 50% FBS for some formulations (Figure 3), especially for the formulation containing 2% DSPE-PEG$_{2000}$-TAT: T% was only about 40%, and then T% increased from 40% to over 60% gradually with the

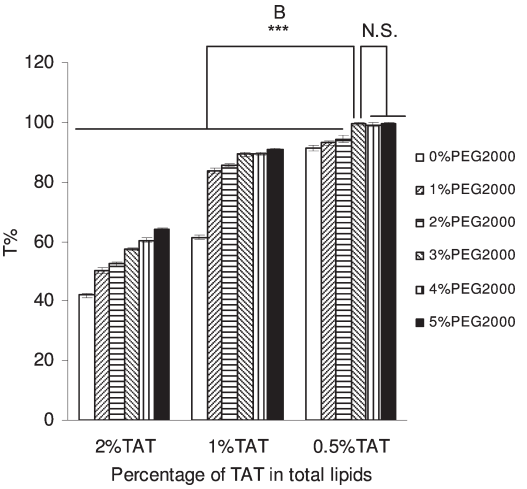

Figure 3. Aggregation characteristic after incubation of different amounts of PEG$_{2000}$ and TAT modified TAT-SL in the presence of 50% FBS at 37 °C for 24 h. The turbidity was indicated by T% which was recorded against blank 50% FBS (T% = 100%). *** = statistically significant differences (p < 0.001); N.S. = no significant difference (n = 3, mean ± SD).

percentage of DPSE-PEG$_{2000}$ increasing from 0% to 5%. When the percentage of DSPE-PEG$_{2000}$-TAT decreased to 1%, T% increased compared with the percentage of 2% DSPE-PEG$_{2000}$-TAT under all DSPE-PEG$_{2000}$ densities. When the percentage of DSPE-PEG$_{2000}$-TAT further decreased to 0.5%, T% could reach a plateau at 3% DSPE-PEG$_{2000}$, nearly 100%, indicating good serum stability for this formulation.

3.3. Cellular Uptake Characteristic *in Vitro*. Efficient cellular uptake plays an important role for the targeted delivery of cargo. The cellular uptake characteristics of different formulations were assessed on C26 cells. The uptake efficiency diminished with the decrease of DSPE-PEG$_{2000}$-TAT; at the same DSPE-PEG$_{2000}$-TAT molar ratio, the uptake efficiency decreased with the increase of DSPE-PEG$_{2000}$ (data not shown), which was opposite with the aggregation trend. When the density of DSPE-PEG$_{2000}$-TAT and DSPE-PEG$_{2000}$ was 0.5% and 3%, respectively, no aggregation occurred (T% was nearly 100%); in addition, this formulation has a higher uptake efficiency than liposomes containing 0.5% DSPE-PEG$_{2000}$-TAT/4% DSPE-PEG$_{2000}$ or 0.5% DSPE-PEG$_{2000}$-TAT/5% DSPE-PEG$_{2000}$;, therefore liposomes containing 0.5% DSPE-PEG$_{2000}$-TAT/3% DSPE-PEG$_{2000}$ made a basic formulation (TAT-SL) for the subsequent experiments.

To test the modulation effect of longer cleavable PEG DSPE-S-S-PEG$_{5000}$ on TAT-SL, various amounts of DSPE-S-S-PEG$_{5000}$ were incorporated into the formulation of TAT-SL. Their uptake characteristics were assessed on C26 in the presence of different amounts of Cys. As shown in Figure 4, the uptake was highly related to the DSPE-S-S-PEG$_{5000}$ density and the concentration of Cys. Briefly, the uptake efficiency of C-TAT-SL diminished from 100.0% to 13.1% of the TAT-SL with the increase of DSPE-S-S-PEG$_{5000}$ from 0% to 8%; at the same percentage of DSPE-S-S-PEG5000, the uptake efficiency increased gradually with the increase of the concentration of Cys. The uptake efficiency of liposomes containing 8% DSPE-S-S-PEG$_{5000}$ could reach a plateau (equivalent to 59.2% of TAT-SL) when the concentration of Cys was between 10 mM and 20 mM.[10]

Before the *in vivo* investigation, the performances of liposomes with various chemical modifications were tested on C26 cells.

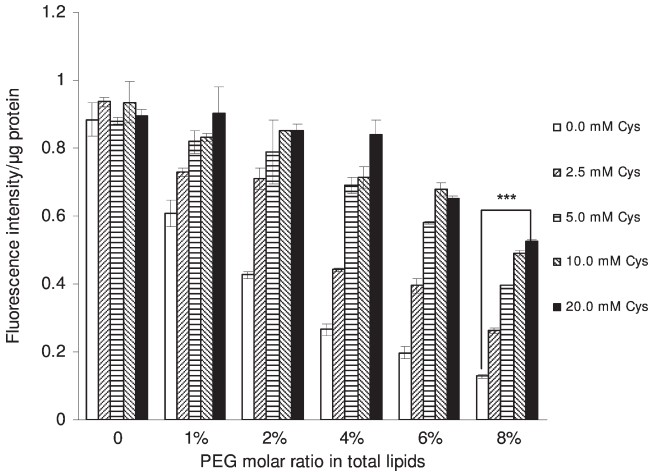

Figure 4. Effects of different amounts of cleavable PEG_{5000} on the uptake of C-TAT-SL (composed of different amounts of cleavable PEG_{5000} and 0.5% TAT + 3% PEG_{2000}) by C26 cells under different concentrations of Cys. *** = statistically significant differences ($p < 0.001$; $n = 3$, mean ± SD).

As shown in Figure 5A,B, the incorporation of 0.5% DSPE-PEG_{2000}-TAT into 3% DSPE-PEG_{2000} modified liposomes could greatly enhance the cellular uptake: the uptake of TAT-SL was over 10 times higher than SL, indicating that the incorporation of TAT was an efficient way to improve the uptake of SL. After the incorporation of 8% DSPE-S-S-PEG_{5000} into the basic formulation of TAT-SL, the uptake was inhibited to quite a low level, and the uptake for liposomes of 8% noncleavable PEG_{5000} + 0.5% TAT + 3% PEG_{2000} (N-TAT-SL) or 8% cleavable PEG_{5000} + 3% PEG_{2000} (C-SL) was also low. After the addition of Cys, the uptake efficiency of C-TAT-SL was over four times ($p < 0.001$) as high as that in the absence of Cys, while no change on the uptake of other formulations was observed, indicating all components of the liposomes worked properly.

The aggregation characteristics of formulations to be used in the *in vivo* experiment were also tested using the same method as described above; no aggregation occurred for all of these formulations even in the presence of Cys (data not shown), indicating these liposomes were quite suitable for the *in vivo* experiments.

3.4. Biodistribution in Tumor-Bearing Mice. The biodistribution of different formulations of liposomes in tumor bearing mice was investigated using an *in vivo* imaging system. As shown in Figure 6, SL accumulated in the tumor clearly. After incorporation of TAT into SL (i.e., TAT-SL), liposomes mainly accumulated in liver with only a minimal distribution in tumor. When 8% DSPE-S-S-PEG_{5000} or 8% DSPE-PEG_{5000} was incorporated into TAT-SL, tumor accumulation was enhanced greatly while liver distribution was diminished and these two formulations had similar biodistribution characteristics, indicating TAT could be shielded by PEG_{5000} during circulation. Besides, through the *in vivo* biodistribution experiments, the peak time range when these liposomes accumulated in tumor was confirmed, that is, between 24 and 48 h postinjection, which was consistent with reported values.[24,40,41] TAT-SL was not used in the subsequent experiments for its nonspecificity and massive liver distribution with minimal tumor accumulation.

3.5. Qualitative and Quantitative Determination of Targeted Delivery Efficiency *in Vivo*. The qualitative determination of targeted delivery efficiency *in vivo* was performed using confocal laser scanning microscopy. As shown in Figure 7, the tumor section from tumor-bearing mice receiving DiD loaded SL, N-TAT-SL, and C-SL showed little red fluorescence (fluorescence of DiD) no matter whether Cys was intravenously administrated or not. C-TAT-SL too showed weak red fluorescence without the intravenous injection of Cys, but with the injection of Cys 24 h post DiD loaded C-TAT-SL injection, it showed strong red fluorescence, indicating that efficient targeted delivery of DiD was achieved by C-TAT-SL in the presence of Cys via systemic administration.

Finally, the delivery efficiency *in vivo* was determined by flow cytometric quantitation of fluorescent dye DiD encapsulated in various formulations of liposomes. As shown in Figure 8, all of the mean fluorescence intensity caused by SL, N-TAT-SL, and C-SL was low both in the absence or presence of Cys, indicating that Cys had no effect on these formulations, whereas the mean fluorescence intensity caused by C-TAT-SL increased by about 48% ($p < 0.001$) compared with SL even in the absence of Cys. After the intravenous injection of Cys, the mean fluorescence intensity of C-TAT-SL was further improved—about 56% ($p < 0.001$) higher than that in the absence of Cys and 130% ($p < 0.001$) higher than other formulations—indicating that an efficient targeted delivery of DiD could be achieved by the combination of C-TAT-SL and Cys via systemic administration.

4. DISCUSSION

The study here aims to develop a liposomal drug delivery system that could highly accumulate in tumor tissue and then transport its cargo into tumor cells efficiently via systemic administration. In our previous study, we confirmed that the combination of TAT and cleavable PEG could exert a synergic role and their *in vivo* performance was evaluated via intratumoral administration.[10] Here, their systemic administration was performed. Before systemic use, the formulation was further optimized to be more suitable for the intravenous injection.

The density of the "functional molecule"—TAT—is highly related to the uptake efficiency and stability of liposomes especially in the presence of high concentration of serum *in vivo*[28] therefore, the density of TAT and protective PEG_{2000} was screened in terms of the aggregation characteristics (indicated by the *T*%) in 50% FBS. Although FBS could not provide a real environment encountered by the liposomes in the blood (in FBS, the effect of blood cells was not considered), this method has already been widely used to test the aggregation characteristics of liposomes,[28] because it might be not the cells but various chemicals (such as proteins) that affected the aggregation of liposmes, and we did observe no difference between the aggregation trend in the absence and in the presence of cells (observed in the cellular uptake experiment in the presence of FBS).

When the aggregation of liposomes occurs in the presence of 50% FBS, the turbidity would increase, and the absorbance (called "*A*" in short) at 750 nm would also increase, while the corresponding *T*% (in a range between 0 and 100%) would decrease, and vice versa. We used *T*% rather than *A* to indicate the turbidity because the former had a wide range and was convenient to record. The transmittance of blank PBS or 50% FBS was set at 100%, and the *T*% of liposomal suspension was normalized by the *T*% of blank PBS or FBS: if the ratio was approximately 100%, it indicated there was no aggregation; if the ratio was far from 100%, it indicated aggregation occurred. We did not use size distribution to measure the aggregation characteristic because, when determining the size by the dynamic scattering

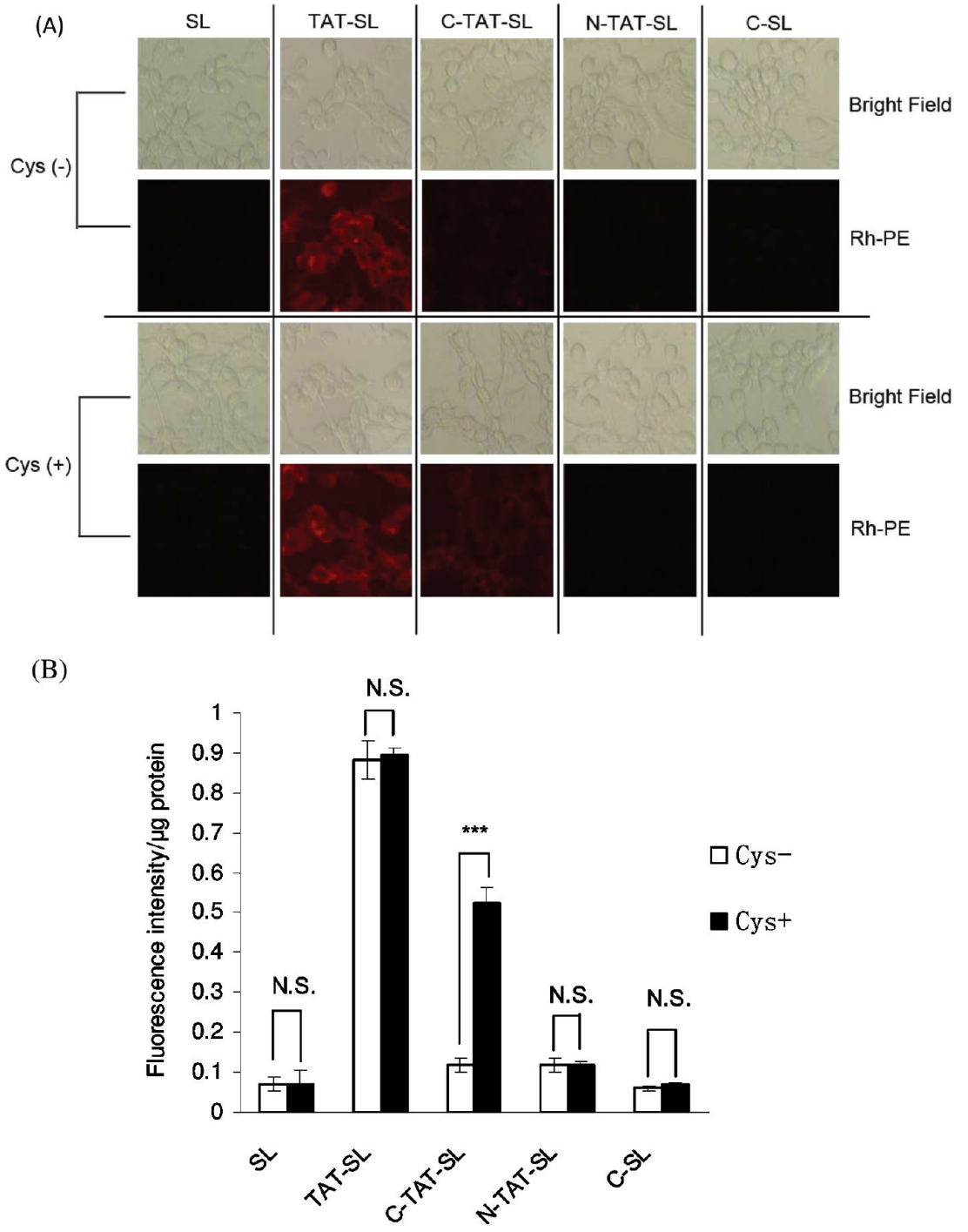

Figure 5. (A) Qualitative observation of uptake of liposomes with various modifications by C26 cells in the absence or presence of Cys *in vitro*. All of these liposomes were labeled by Rh-PE. (B) Quantitative determination of uptake characteristics of liposomes with various modifications by C26 cells in the absence or presence of Cys *in vitro*. *** = statistically significant differences ($p < 0.001$); N.S. = no significant difference ($n = 3$, mean ± SD).

laser (DLS) method, we found the result was unreliable—the average size determined would still be around 100 nm even if severe aggregation occurred, which was contradicted with the phenomenon we observed.

The aggregation became aggravated when the density of TAT increased from 0.5% to 2%; at the same density of TAT, the aggregation trend diminished with the increase of DSPE-PEG_{2000}. This may be caused by the positive charge of TAT peptide (as shown in Table 1), which could interact with proteins in the serum, and then aggregation occurred, while the incorporation of protective DSPE-PEG_{2000} could alleviate the aggregation due to the hydrophilic properties and steric stabilization. Liposomes containing 0.5% DSPE-PEG_{2000}-TAT and 3% DSPE-PEG_{2000} were made as the basic formulation (TAT-SL) for the subsequent experiments because at this TAT density, *T*% could reach plateau (nearly 100%) when 3% DSPE-PEG_{2000} was incorporated,

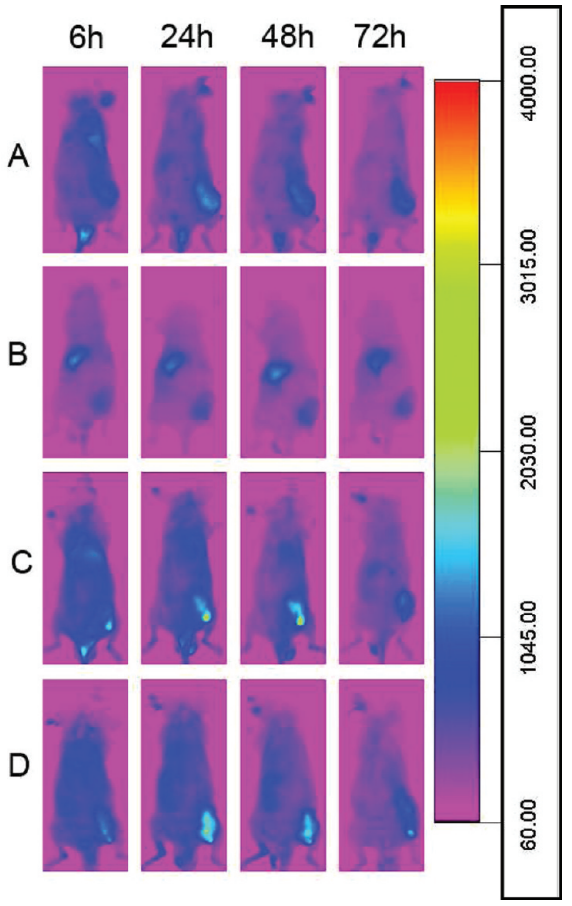

Figure 6. Biodistribution of different formulations of DiR loaded liposomes in C26 tumor-bearing mice at different time points. The optical image was taken by Kodak In-Vivo FX Professional Imaging System (New Haven, CT) with a wavelength set at Ex = 770 nm, Em = 830 nm and an exposure time of 20 s. A: SL, B: TAT-SL, C: C-TAT-SL, D: N-TAT-SL.

as stable as the higher density of DSPE-PEG_{2000} (4% and 5%) modified liposomes, indicating no aggregation occurred, while the uptake efficiency of liposomes containing 0.5% DSPE-PEG_{2000}-TAT + 3% DSPE-PEG_{2000} was higher than that of liposomes containing 0.5% DSPE-PEG_{2000}-TAT + 4% DSPE-PEG_{2000} or 5% DSPE-PEG_{2000}. Besides, it was reported that a PEG_{2000} density higher than 2% could endue the liposomes with long circulating properties *in vivo*,[42] which could be used as control (stealth liposomes) in the subsequent experiments.

The modulation effect of cleavable PEG_{5000} on the basic formulation (TAT-SL) was evaluated with various amounts of DSPE-S-S-PEG_{5000} incorporated. As a result, the uptake characteristic was consistent with our previous research: the higher

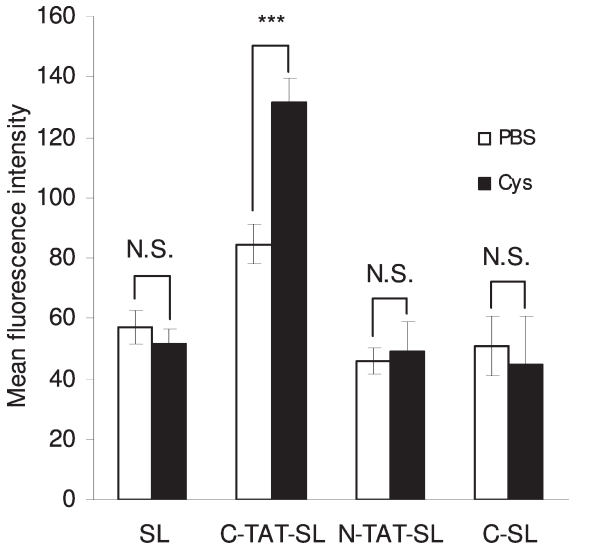

Figure 8. Cytometric quantitation of cell suspensions from tumor-bearing mice receiving different formulations of DiD loaded liposomes ($n = 3$, mean ± SD). *** = statistically significant differences ($p < 0.001$); N.S. = no significant difference.

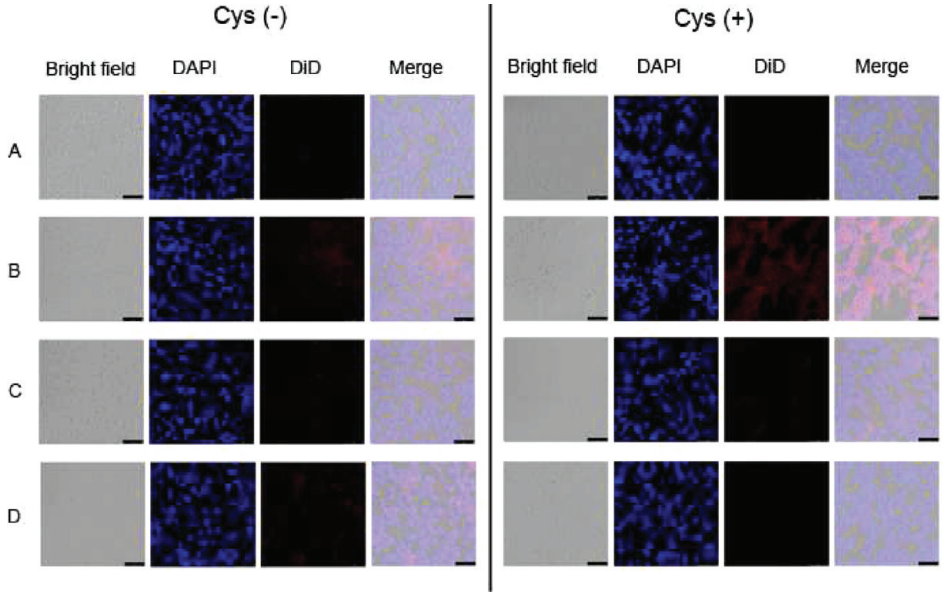

Figure 7. CLSM images of C26 tumor frozen sections from tumor-bearing mice receiving different formulations of DiD loaded liposomes. A: SL, B: C-TAT-SL, C: N-TAT-SL, D: C-SL. In each set from left to right: bright field, DAPI, DiD, merge.

the density of DSPE-S-S-PEG$_{5000}$ incorporated, the lower uptake efficiency it had; at the same density of DSPE-S-S-PEG$_{5000}$, the uptake efficiency increased with the increase of Cys concentration. These characteristics indicated that cleavable PEG was in good response to the Cys.

Various formulations of liposomes to be used *in vivo* were tested *in vitro* in advance in terms of uptake characteristics and stability in the presence of 50% FBS. As a result SL, TAT-SL, C-TAT-SL, N-TAT-SL, and C-SL showed good stability in the presence of 50% FBS (no aggregation occurred), even in the presence of Cys (data not shown). TAT-SL showed efficient uptake compared with SL, while SL, N-TAT-SL, and C-SL showed low uptake no matter in the absence or presence of Cys, and C-TAT-SL too showed low uptake in the absence of Cys, but in the presence of Cys, the uptake of C-TAT-SL was over 4 times ($p < 0.001$) as high as that in the absence of Cys. These characteristics indicated all of the functional materials worked properly, which provided good assurance for the *in vivo* experiments. The uptake characteristics of DiD loaded liposomes were parallel with Rh-PE labeled liposomes (see Supporting Information).

The *in vivo* experiments were performed on a murine solid tumor/C26 tumor-bearing mice, which had good vascular permeability within tumor tissue and a typical EPR effect.[32] A noninvasive optical imaging system was used to investigate the distribution of DiR loaded liposomes, and thus the fate of liposomes *in vivo* could be monitored conveniently and continuously. DiR was used as the fluorescence probe because it could be stably encapsulated into liposomes easily. In addition, the excitation and emission wavelength of DiR was in a range of 700−900 nm belonging to the near-infrared (NIR) spectrum, within which light could penetrate deeply into tissue, and background from tissue autofluorescence and absorption from intrinsic chromophore were low.[34]

The distribution of liposomes between the tumor and the liver was a competitive process. As shown in Figure 6, SL exhibited obvious tumor accumulation when 0.5% DSPE-PEG$_{2000}$-TAT was incorporated into SL (i.e., TAT-SL). Most of the liposomes were distributed in the liver with only minimal tumor accumulation; the reason for this might be that the positively charged TAT readily bind to the opsonin in serum and then liposomes were trapped by the liver. The incorporation of cleavable PEG$_{5000}$ or noncleavable PEG$_{5000}$ into TAT-SL could diminish the liver distribution and increase the tumor accumulation greatly as positively charged TAT could be shielded by longer PEG$_{5000}$;[15] thus the binding of opsonin was inhibited. It is also reported that a high density of PEG is favorable for the passive tumor accumulation, because high density of PEG will be favorable for the RES escape by shielding the surface of liposomes.[43] Compared with SL (containing 3% DSPE-PEG$_{2000}$), N-TAT-SL and C-TAT-SL had a higher density of PEG (3% DSPE-PEG$_{2000}$ + 8% PEG$_{5000}$) which could shield the surface of the liposomes much better, thus reducing the chance of being recognized by opsonin and uptaken by liver and increasing the accumulation in tumor tissue.[43] Besides, C-TAT-SL and N-TAT-SL had similar distribution characteristics, and the peak time of tumor accumulation was between 24 and 48 h, indicating the long circulating properties of DSPE-S-S-PEG$_{5000}$ indirectly.

Although the high density of surface PEG is unfavorable for the stability of liposomes, the highest PEG density that could be used in liposomes varied in different circumstances.[8,43] When C-TAT-SL (containing 3% DSPE-PEG$_{2000}$ + 8% PEG$_{5000}$) was prepared, it was still stable. The reason for this might be that the PEG material was added in the lipid film before hydration and the PEG was randomly distributed both on both interior surface and exterior surface of liposomes once they were formed, that is to say the surface PEG density might be only about 5% or so, and besides, cholesterol in the lipid bilayer could also help stabilize it. However, to further increase the surface density of PEG special technology may be needed such as charge−charge interaction between the core and the lipid bilayer, which has been successfully used in the preparation of LPD by Li and Huang.[43]

For the intracellular delivery *in vivo*, an analogue of DiR, DiD, was used for the fluorescence probe for its wavelength of Ex and Em of 644 nm and 665 nm, respectively, which was much more suitable than DiR for the detection by confocal laser scanning microscopy and flow cytometry. DiD-loaded liposomes were intravenously injected into tumor-bearing mice; after the maximal tumor accumulation was achieved, Cys in PBS was intravenously injected at a safe dose to cleave PEG$_{5000}$ from liposomes as reported previously,[24] using blank PBS as a control. The time point when Cys should be injected did play an important role. As shown in Figure 6, the peak time for the accumulation was between 24 and 48 h, which was consistent with the previous report. If Cys was injected too early (less than 24 h), there would not be enough liposomes in tumor region, and high nonspecific uptake of C-TAT-SL by the liver would occur because of the cleavage of PEG caused by the exogenous Cys in the bloodstream; if Cys was injected too late (more than 48 h), most of C-TAT-SL might have been cleared from the tumor region due to the weak tumor−liposome association. Cys was injected at 24 h rather than 48 h, because the accumulation of C-TAT-SL was comparable between the two time points, and there would be more time for C-TAT-SL to interact with the tumor cells in the form of TAT-SL after it was activated at 24 h before being cleared from the tumor region, which is helpful for the efficient delivery of cargo into tumor cells. Although residual C-TAT-SL in the bloodstream could also be activated and then interact with normal cells nonspecifically, a considerable amount of injected C-TAT-SL has been accumulated in tumor region at 24 h, and most of the residual C-TAT-SL in the blood could be increasingly eliminated by the liver after it was activated (see the biodistribution of TAT-SL), thus reducing the side effects caused by the excessive contact of liposomes with normal tissue.[12]

The tumor frozen section showed that SL, N-TAT-SL, and C-SL had little red fluorescence (fluorescence of DiD) no matter in the presence of Cys or not. Although the tumor accumulation of N-TAT-SL was considerable, the signal of DiD was not found in the tumor section, which might be caused by the easy loss of liposomes from the extracellular space within the tumor tissue during the tumor section preparation (such as repeated PBS wash). C-TAT-SL too showed weak red fluorescence in the absence of Cys, but in the presence of Cys, C-TAT-SL exhibited obvious red fluorescence, indicating the successful delivery of DiD by the combination of C-TAT-SL and Cys.

It is hypothesized that the injection of Cys would increase the retentoin of C-TAT-SL in the tumor region due to the increased association between C-TAT-SL and tumor cells caused by the cleavage of PEG. However, when following up the accumulation of C-TAT-SL after injecting Cys at 24 h, we did not observe a great increase of accumulation compared with the accumulation in the absence of Cys (see the Supporting Information), although a small increase could be observed. The reason might be the difference caused by the fact that the injection of Cys could not

be observed clearly by using the optical imaging system. It is necessary to quantify the uptake of C-TAT-SL in the entire tumor region to confirm its function, which may also make up for the shortage of qualitative analysis such as a tumor section that could only exhibit the local uptake within the tumor tissue.

To learn the uptake of liposomes in vivo quantitatively, the entire tumor tissue was excised and dissipated into tumor cell suspension using the dissociation solution, then determined by the flow cytometry. Cells dissociated from tumor tissue containing both endothelial cells and tumor cells were not discriminated, and the total uptake efficiency was determined because TAT could penetrate both of these cells.[20] As shown in Figure 8, the delivery of SL, N-TAT-SL, and C-SL *in vivo* was weak no matter with the injection of Cys or not, but the delivery of C-TAT-SL showed an average increase of 48% ($p < 0.001$) compared with the rest three formulations even in the absence of Cys. C-TAT-SL with a subsequent injection of Cys further improved the delivery efficiency—about 56% ($p < 0.001$) higher than C-TAT-SL without the injection of Cys and 130% ($p < 0.001$) higher than the three other formulations. The reason might be that the gradual cleavage of DSPE-S-S-PEG_{5000} occurred during circulation although the concentration of reducing agent *in vivo* was always low (8 μM cysteine and 2 μM glutathione),[44] and minimal cleavage in the DSPE-S-S-PEG_{5000} density could lead to an increase of uptake by cells (Figure 5); besides, some reducing substance such as surface-associated redox enzymes on the membrane of tumor cells might also boost the cleavage of PEG and facilitate the uptake of liposomes.[44] In spite of the probable cleavage of DSPE-S-S-PEG *in vivo*, it could still endue the liposome with long circulation properties, because residual PEG_{5000} on the surface of C-TAT-SL was still considerable, and that liposomes modified with DSPE-S-S-PEG_{5000} had similar distribution characteristics with DSPE-PEG_{5000} (a noncleavable PEG_{5000} *in vivo*) modified liposomes was an evidence.

The cleavage of PEG *in vivo* in a safe way has been reported previously—that is, the intravenous injection of Cys. Unlike other reducing agents such as DTT which has some toxicity, Cys itself is existent in human body, and 120 mg/kg Cys was reported to be innocuous for the *in vivo* use.[24] However, the accurate concentration of Cys in the extracellular space within the tumor tissue was hard to determine, but from the increase of delivery efficiency *in vivo* with the administration of Cys, its presence in the tumor tissue could be confirmed indirectly. Although Cys was widely distributed *in vivo* after intravenous injection, C-TAT-SL has been concentrated in tumor tissue in advance via the EPR effect, and the delivery of liposomal cargo would still mainly occur in tumor tissue. Thus side effects on other organs were minimal. Cys as a small molecule might not stay too long in the tumor region, but we had *in vitro* evidence that Cys could result in adequate removal of PEG even in less than 4 h (see the Supporting Information), which is also reported elsewhere.[24]

So far, although the passive targeted liposomes such as Doxil could accumulate in tumor tissue via the EPR effect, it had weak association with tumor cells, therefore limiting its efficacy.[12] Besides, even though active targeting such as grafting ligand to the surface of liposome could increase the uptake both *in vitro* and *in vivo*, it also encounters a challenge, because the incorporation of ligands to the liposome may compromise its long circulating properties due to the recognization of opsonin, thus reducing its passive accumulation in the tumor region.[2,24] Compared with the above targeting strategies, TAT and cleavable PEG comodified liposomes had special advantages, because PEG could shield TAT, thus reducing the chance of being recognized by opsonin and increasing the passive accumulation in tumor region. When the accumulation of liposomes have reached plateau, exogenous Cys could cleave PEG, and then the exposed TAT could mediate the internalization of liposomes with high efficiency. In this way, maximal tumor accumulation and efficient uptake by tumor cells can be achieved simultaneously.[2]

5. CONCLUSIONS

The TAT and cleavable PEG comodified liposomal delivery system that has been optimized here was used in the systemic administration successfully. The incorporation of TAT enhanced the cellular uptake efficiency *in vitro*, but the distribution in the tumor was greatly decreased with an obvious liver accumulation *in vivo*. Simultaneous incorporation of cleavable PEG_{5000} and TAT (C-TAT-SL) could increase the tumor accumulation with a low distribution in the liver, which had similar distribution profiles with the noncleavable PEG_{5000} and TAT comodified liposomes (N-TAT-SL). The delivery efficiency of C-TAT-SL *in vivo* was also higher than other formulations, especially with the intravenous injection of Cys at 24 h postliposome injection, about 130% higher than SL. Such a combination of C-TAT-SL and Cys could highly accumulate its cargo in tumor tissue and then transport them into tumor cells efficiently, which is useful in keeping the advantages of PEG and TAT and overcoming the nonspecificity of TAT and shortages of PEG in hindering the interaction between cells and liposomes, and is therefore quite a promising drug delivery system in tumor diagnosis and treatment in the future.

■ ASSOCIATED CONTENT

Supporting Information. Uptake of different formulations of DiD loaded liposomes by C26 cells determined qualitatively and quantitatively. This material is available free of charge via the Internet at http://pubs.acs.org.

■ AUTHOR INFORMATION

Corresponding Author

*Mailing address: West China School of Pharmacy, Sichuan University, No. 17 Block 3 Southern Renmin Road, Chengdu, Sichuan, 610041, China. Tel./Fax: +86-28-85502532. E-mail: qinhe@scu.edu.cn.

Author Contributions

§These authors contributed equally to this work.

■ ACKNOWLEDGMENT

The work was funded by the National Natural Science Foundation of China (30873166, 81072599), the State Key Program of National Natural Science of China (81130060), the National Basic Research Program of China (2007CB935801, 2009CB903300), and the Ph.D. Programs Foundation of the Ministry of Education of China (20090181110083). The authors thank Zhenlei Song for providing help on the synthesis of cleavable PEG and other compounds. We acknowledge Chunmeng Shi and Yongping Su from the Institute of Combined Injury in the third Military Medical University for providing equipment for the optical imaging, and we also acknowledge Philippe Rizo and Pierre-Alix Dancer from Fluoptics for their help on the optical imaging.

REFERENCES

(1) Byrne, J.; Betancourt, T.; Brannon-Peppas, L. Active targeting schemes for nanoparticle systems in cancer therapeutics. *Adv. Drug Delivery Rev.* **2008**, *60*, 1615–1626.

(2) Gullotti, E.; Yeo, Y. Extracellularly Activated Nanocarriers: A New Paradigm of Tumor Targeted Drug Delivery. *Mol. Pharmaceutics* **2009**, *6*, 1041–1051.

(3) Lammers, T.; Hennink, W.; Storm, G. Tumour-targeted nanomedicines: principles and practice. *Br. J. Cancer* **2008**, *99*, 392–397.

(4) Misra, R.; Acharya, S.; Sahoo, S. Cancer nanotechnology: application of nanotechnology in cancer therapy. *Drug Discovery Today* **2010**, *15*, 842–850.

(5) Shin, D. Application of Nanotechnology in Cancer Therapy and Imaging. *Drug Metab. Rev.* **2010**, *42*, 13–13.

(6) Torchilin, V. Targeted pharmaceutical nanocarriers for cancer therapy and Imaging. *AAPS J.* **2007**, *9*, E128–E147.

(7) Wang, M.; Thanou, M. Targeting nanoparticles to cancer. *Pharmacol. Res.* **2010**, *62*, 90–99.

(8) Sawant, R.; Hurley, J.; Salmaso, S.; Kale, A.; Tolcheva, E.; Levchenko, T.; Torchilin, V. "SMART" drug delivery systems: Double-targeted pH-responsive pharmaceutical nanocarriers. *Bioconjugate Chem.* **2006**, *17*, 943–949.

(9) Maeda, T.; Fujimoto, K. A reduction-triggered delivery by a liposomal carrier possessing membrane-permeable ligands and a detachable coating. *Colloids Surf., B* **2006**, *49*, 15–21.

(10) Kuai, R.; Yuan, W.; Qin, Y.; Chen, H.; Tang, J.; Yuan, M.; Zhang, Z.; He, Q. Efficient Delivery of Payload into Tumor Cells in a Controlled Manner by TAT and Thiolytic Cleavable PEG Co-Modified Liposomes. *Mol. Pharmaceutics* **2010**, *7*, 1816–1826.

(11) Gabizon, A.; Goren, D.; Horowitz, A.; Tzemach, D.; Lossos, A.; Siegal, T. Long-circulating liposomes for drug delivery in cancer therapy: A review of biodistribution studies in tumor-bearing animals. *Adv. Drug Delivery Rev.* **1997**, *24*, 337–344.

(12) Li, S.; Huang, L. Stealth nanoparticles: High density but sheddable PEG is a key for tumor targeting. *J. Controlled Release* **2010**, *145*, 178–181.

(13) Fretz, M.; Koning, G.; Mastrobattista, A.; Jiskoot, W.; Storm, G. OVCAR-3 cells internalize TAT-peptide modified liposomes by endocytosis. *Biochim. Biophys. Acta, Biomembr.* **2004**, *1665*, 48–56.

(14) Pappalardo, J.; Quattrocchi, V.; Langellotti, C.; Di Giacomo, S.; Gnazzo, V.; Olivera, V.; Calamante, G.; Zamorano, P.; Levchenko, T.; Torchilin, V. Improved transfection of spleen-derived antigen-presenting cells in culture using TATp-liposomes. *J. Controlled Release* **2009**, *134*, 41–46.

(15) Torchilin, V.; Rammohan, R.; Weissig, V.; Levchenko, T. TAT peptide on the surface of liposomes affords their efficient intracellular delivery even at low temperature and in the presence of metabolic inhibitors. *Proc. Natl. Acad. Sci. U.S.A.* **2001**, *98*, 8786–8791.

(16) Torchilin, V. Tat peptide-mediated intracellular delivery of pharmaceutical nanocarriers. *Adv. Drug Delivery Rev.* **2008**, *60*, 548–558.

(17) Torchilin, V.; Levchenko, T.; Rammohan, R.; Volodina, N.; Papahadjopoulos-Sternberg, B.; D'Souza, G. Cell transfection in vitro and in vivo with nontoxic TAT peptide-liposome-DNA complexes. *Proc. Natl. Acad. Sci. U.S.A.* **2003**, *100*, 1972–1977.

(18) Vandenbroucke, R.; De Smedt, S.; Demeester, J.; Sanders, N. Cellular entry pathway and gene transfer capacity of TAT-modified lipoplexes. *Biochim. Biophys. Acta, Biomembr.* **2007**, *1768*, 571–579.

(19) Romberg, B.; Hennink, W.; Storm, G. Sheddable coatings for long-circulating nanoparticles. *Pharm. Res.* **2008**, *25*, 55–71.

(20) Vives, E.; Schmidt, J.; Pelegrin, A. Cell-penetrating and cell-targeting peptides in drug delivery. *Biochim. Biophys. Acta, Rev. Cancer* **2008**, *1786*, 126–138.

(21) Hatakeyama, H.; Ito, E.; Akita, H.; Oishi, M.; Nagasaki, Y.; Futaki, S.; Harashima, H. A pH-sensitive fusogenic peptide facilitates endosomal escape and greatly enhances the gene silencing of siRNA-containing nanoparticles in vitro and in vivo. *J. Controlled Release* **2009**, *139*, 127–132.

(22) Hatakeyama, H.; Akita, H.; Kogure, K.; Oishi, M.; Nagasaki, Y.; Kihira, Y.; Ueno, M.; Kobayashi, H.; Kikuchi, H.; Harashima, H. Development of a novel systemic gene delivery system for cancer therapy with a tumor-specific cleavable PEG-lipid. *Gene Ther.* **2007**, *14*, 68–77.

(23) Kale, A.; Torchilin, V. Enhanced transfection of tumor cells in vivo using "Smart" pH-sensitive TAT-modified pegylated liposomes. *J. Drug Targeting* **2007**, *15*, 538–545.

(24) McNeeley, K.; Karathanasis, E.; Annapragada, A.; Bellamkonda, R. Masking and triggered unmasking of targeting ligands on nanocarriers to improve drug delivery to brain tumors. *Biomaterials* **2009**, *30*, 3986–3995.

(25) Mok, H.; Bae, K.; Ahn, C.; Park, T. PEGylated and MMP-2 Specifically DePEGylated Quantum Dots: Comparative Evaluation of Cellular Uptake. *Langmuir* **2009**, *25*, 1645–1650.

(26) Terada, T.; Iwai, M.; Kawakami, S.; Yamashita, F.; Hashida, M. Novel PEG-matrix metalloproteinase-2 cleavable peptide-lipid containing galactosylated liposomes for hepatocellular carcinoma-selective targeting. *J. Controlled Release* **2006**, *111*, 333–342.

(27) Xu, H.; Deng, Y.; Chen, D.; Hong, W.; Lu, Y.; Dong, X. Esterase-catalyzed dePEGylation of pH-sensitive vesicles modified with cleavable PEG-lipid derivatives. *J. Controlled Release* **2008**, *130*, 238–245.

(28) Maeda, N.; Takeuchi, Y.; Takada, M.; Sadzuka, Y.; Namba, Y.; Oku, N. Anti-neovascular therapy by use of tumor neovasculature-targeted long-circulating liposome. *J. Controlled Release* **2004**, *100*, 41–52.

(29) Cryan, S.; Devocelle, M.; Moran, P.; Hickey, A.; Kelly, J. Increased intracellular targeting to airway cells using octaarginine-coated liposomes: In vitro assessment of their suitability for inhalation. *Mol. Pharmaceutics* **2006**, *3*, 104–112.

(30) Chang, Y.; Chang, C.; Yu, C.; Chang, T.; Chen, L.; Chen, M.; Lee, T.; Ting, G. Therapeutic efficacy and microSPECT/CT imaging of Re-188-DXR-liposome in a C26 murine colon carcinoma solid tumor model. *Nucl. Med. Biol.* **2010**, *37*, 95–104.

(31) Rossi, J.; Giasson, S.; Khalid, M.; Delmas, P.; Allen, C.; Leroux, J. Long-circulating poly(ethylene glycol)-coated emulsions to target solid tumors. *Eur. J. Pharm. Biopharm.* **2007**, *67*, 329–338.

(32) Ogawara, K.; Un, K.; Minato, K.; Tanaka, K.; Higaki, K.; Kimura, T. Determinants for in vivo anti-tumor effects of PEG liposomal doxorubicin: Importance of vascular permeability within tumors. *Int. J. Pharm.* **2008**, *359*, 234–240.

(33) Larkin, J.; Soden, D.; Collins, C.; Tangney, M.; Preston, J.; Russell, L.; McHale, A.; Dunne, C.; O'Sullivan, G. Combined electric field and ultrasound therapy as a novel anti-tumour treatment. *Eur. J. Cancer* **2005**, *41*, 1339–1348.

(34) Zhang, C.; Liu, T.; Su, Y.; Luo, S.; Zhu, Y.; Tan, X.; Fan, S.; Zhang, L.; Zhou, Y.; Cheng, T.; Shi, C. A near-infrared fluorescent heptamethine indocyanine dye with preferential tumor accumulation for in vivo imaging. *Biomaterials* **2010**, *31*, 6612–6617.

(35) Ghoroghchian, P.; Therien, M.; Hammer, D. In vivo fluorescence imaging: a personal perspective. *Wiley Interdiscip. Rev.: Nanomed. Nanobiotechnol.* **2009**, *1*, 156–167.

(36) Song, S.; Liu, D.; Peng, J.; Sun, Y.; Li, Z.; Gu, J.; Xu, Y. Peptide ligand-mediated liposome distribution and targeting to EGFR expressing tumor in vivo. *Int. J. Pharm.* **2008**, *363*, 155–161.

(37) Goutayer, M.; Dufort, S.; Josserand, V.; Royere, A.; Heinrich, E.; Vinet, F.; Bibette, J.; Coll, J.; Texier, I. Tumor targeting of functionalized lipid nanoparticles: Assessment by in vivo fluorescence imaging. *Eur. J. Pharm. Biopharm.* **2010**, *75*, 137–147.

(38) Abu Lila, A.; Doi, Y.; Nakamura, K.; Ishida, T.; Kiwada, H. Sequential administration with oxaliplatin-containing PEG-coated cationic liposomes promotes a significant delivery of subsequent dose into murine solid tumor. *J. Controlled Release* **2010**, *142*, 167–173.

(39) Kirpotin, D.; Drummond, D.; Shao, Y.; Shalaby, M.; Hong, K.; Nielsen, U.; Marks, J.; Benz, C.; Park, J. Antibody targeting of long-circulating lipidic nanoparticles does not increase tumor localization but does increase internalization in animal models. *Cancer Res.* **2006**, *66*, 6732–6740.

(40) Hong, R.; Huang, C.; Tseng, Y.; Pang, V.; Chen, S.; Liu, J.; Chang, F. Direct comparison of liposomal doxorubicin with or without

polyethylene glycol coating in C-26 tumor-bearing mice: Is surface coating with polyethylene glycol beneficial? *Clin. Cancer Res.* **1999**, *5*, 3645–3652.

(41) Siegal, T.; Horowitz, A.; Gabizon, A. Doxorubicin encpsulated in sterically stabilized liposomes for the treatment of a brain tumor model - biodistribution and therapeautic efficacy. *J. Neurosurg.* **1995**, *83*, 1029–1037.

(42) Dos Santos, N.; Allen, C.; Doppen, A.; Anantha, M.; Cox, K.; Gallagher, R.; Karlsson, G.; Edwards, K.; Kenner, G.; Samuels, L.; Webb, M.; Bally, M. Influence of poly(ethylene glycol) grafting density and polymer length on liposomes: Relating plasma circulation lifetimes to protein binding. *Biochim. Biophys. Acta, Biomembr.* **2007**, *1768*, 1367–1377.

(43) Li, S.; Huang, L. Nanoparticles evading the reticuloendothelial system: Role of the supported bilayer. *Biochim. Biophys. Acta, Biomembr.* **2009**, *1788*, 2259–2266.

(44) Saito, G.; Swanson, J.; Lee, K. Drug delivery strategy utilizing conjugation via reversible disulfide linkages: role and site of cellular reducing activities. *Adv. Drug Delivery Rev.* **2003**, *55*, 199–215.